Frequency Dependent Chaos in a Single CMOS Inverter: Two Related Perspectives

Sai Venkatesh Balasubramanian

Sree Sai Vidhya Mandhir, Mallasandra, Bengaluru-560109, Karnataka, India.
saivenkateshbalasubramanian@gmail.com

Abstract

The generation of Chaos in Electronics has largely been implemented using the Chua circuits, where the initial conditions are described by system parameters such as resistors and capacitors. The present work provides a radical shift in approach by proposing signal based chaos generators. The essential design here is the coupling of two sinusoidal signal sources to a CMOS inverter circuit, which is seen to exhibit nonlinear behavior thanks to its transfer characteristics and non-quasi static behavior. The Standard Circle Map, ideally suited to describing nonlinear coupling of oscillations with competing frequencies is studied and a 'frequency map' is derived from it. The latter is studied using bifurcation and cobweb plots. A second perspective, the amplitude map is created by forming a difference equation using the CMOS inverter transfer function. This map is explored using the bifurcation plots and phase portraits. Finally, the proposed design is implemented experimentally and the generated chaotic output is validated using phase portraits and Fourier spectra. The effect of driving frequency on the output is characterized using Kolmogorov Entropy and Lyapunov Exponents, giving rise to the term 'Frequency Dependent Chaos'. The fresh perspectives of a signal oriented chaos discussed in the present work exhibits the advantages of simple circuitry and easy tunability, and this forms the novelty of the present work.

Keywords: Chaos Generation, Frequency Dependent Chaos, Standard Circle Map, Bifurcation Analysis, CMOS Inverter

1. Introduction

Chaos Theory, the hallmark of Nonlinear Science has grown in leaps and bounds over the past decade, thanks to the development in computer simulations and visualizations of abstract mathematical equations and iterative maps, using which, beautiful and ornamental patterns of long term evolutions depicting various aspects of nature have been accessible for the first time ever [1, 2, 3, 4, 5, 6, 7, 8]. The key defining aspects of chaos are determinism, dynamic behavior and an extreme sensitivity to initial conditions, quantified by measures such as the Lyapunov Exponent [3, 4]. Consequently, diverse applications of chaos theory have emerged, some of which involve biology, astronomy, engineering and meteorology [3, 4, 9, 10, 11, 12, 13, 14, 15, 16, 17].

Applications of chaos are not limited to the basic sciences alone: In the information technology domain, chaos theory has been used for secure communication and computing purposes [18, 19, 20, 21, 22, 23]. Moreover, in the field of electronics, the discovery and design of the Chua's Diode and other associated circuits have enabled tremendous progress in chaos generation and synchronization applications [24]. However, most of these circuits being op-amp based realizations of nonlinear differential equations, implement the initial conditions at a system level, such as the Resistor and Capacitor values in the Chua Oscillator, for instance [24, 25, 26, 27, 28]. Apart from causing power dissipation, it also poses problems pertaining to ease of tunability when implemented at an IC level operating at high frequencies [29]. A more convenient alternative would involve determining and manipulating the initial conditions from a signal level, in driven chaotic systems realized using simple circuitry.

That is the key motivation behind the present work, which pertains to a signal oriented chaos generation in a single CMOS Inverter, which is the simplest circuit unit in most state-of-the-art CMOS Technologies [29]. Firstly, the two factors contributing to the nonlinearity seen in a MOS Transistor, namely DC Characteristics and Non-Quasi Static Effect are explored [30, 31, 32, 33, 34, 35]. The fundamental backbone in the proposed chaos generator is the coupling of two sinusoidal sources to a CMOS Inverter. Thus, in this light, the standard circle map, an iterative map known to model nonlinear interactions of oscillations at two competing frequencies, is explored, and a 'frequency map' is adapted from it using simple manipulations, with the control parameter being the frequency ratio between the two driving signals [36, 37, 38, 39, 40]. This Frequency Map forms the first perspective and is studied using bifurcation plots and cobweb plots. Following this, the second perspective is introduced. Here, the transfer function of a typical CMOS inverter in 180nm CMOS Technology is fitted to a sigmoid, and using this, a difference equation depicting the CMOS Inverter output

$$I_d = \frac{\mu_n Z C_i}{L}\left[\left(V_G - V_{FB} - 2\psi_f - \frac{V_D}{2}\right)V_D - \frac{2}{3}\frac{\sqrt{2\epsilon j_s q N_a}}{C_i}\left[(V_D + 2\psi_f)^{1.5} - (2\psi_f)^{1.5}\right]\right] \tag{1}$$

for a coupled sinusoidal input is formed. This difference equation is adapted to an iterative map, termed the 'Amplitude Map'. The amplitude map is studied using bifurcation and phase portraits. Finally, a hardware implementation of the CMOS Inverter is performed, and the generated chaotic output is studied using the phase portraits and FFT Spectra. It is found that the inferences obtained from the theoretical formulation of the frequency and amplitude maps agree with the observed results. Finally the effect of frequency ratio on the nature of generated chaos is studied using standard chaotic characterization techniques such as Lyapunov Exponents and Kolmogorov Entropy [41, 42].

The formulations of the frequency dependent chaos discussed in the present work offer a radically different and fresh perspective on the generation chaos - a transition from system oriented chaos generation to signal oriented chaos generation. This enables the design of chaos generators to be achieved with extremely simple circuitry, which translates to less power dissipation. Thus, the signal oriented chaos formulation coupled with the simplicity of design form the novelty of the present work.

2. Nonlinearity in CMOS Transistors

It is well known that the most essential criteria in the generation of most types of chaos is nonlinearity. In the present work, this criteria is satisfied by the nonlinear behavior of the Metal-Oxide Semiconductor Field Effect Transistor (MOSFET), which is a result of two contributing factors which are discussed below.

1. **Nonlinearity in the Output Characteristics**: This factor primarily owes to the three regions of MOSFET operation (cutoff, linear and saturation) and the transitions between them [32, 33]. This nonlinear behavior is best understood by studying the current-voltage characteristics encompassing both linear and saturation regions, and given by Equation 1 [30]. In this equation, μ_n denotes the electron mobility, C_i the intrinsic capacitance, V_{FB} is the flat band voltage, j_s is the current density, q is the charge, N_a is the acceptor concentration, ψ_f denotes the work function, L denotes the channel length and Z denotes the channel width, both of which are the key transistor geometry parameters. This nonlinear behavior can be witnessed in the I-V characteristics of typical NMOS and PMOS transistors sized to $2\lambda \times 4\lambda$ in 180nm CMOS Technology, as shown in Fig. (1) and Fig. (2).

2. **Non-Quasi Static (NQS) Behavior**: Significant at high operating frequencies, the non-quasi static charge model of the MOS channel states that the channel of a MOSFET can be modeled as a nonlinear transmission line [31, 34]. An illustration of the NQS model applied to the NMOSFET along with the drain, gate and source capacitances is shown in Fig.(3). The equivalent representation of the nonlinear transmission line is seen as an Elmore resistance, which is length dependent and indicates the effect of wiring and transistor geometry in generation of chaos [31, 34]. This equivalent circuit with the Elmore resistance denoted by 'Re' is also shown in Fig.(3). The dependence on the Elmore Resistance on the gate-source voltage V_{gs} is given as follows [31, 34]:

$$Re = \frac{L_{eff}}{10\mu_{eff}W_{eff}C_{ox}(V_{gs} - V_{th})} \tag{2}$$

where μ_{eff} is the effective carrier mobility, L_{eff} and W_{eff} denote the effective channel length and width of the NMOS transistor, C_{ox} denotes the oxide layer capacitance and V_{th} is the threshold voltage of the transistor. The significance of the application of this Elmore Resistance to the Non-Quasi Static model is that the NQS Relaxation time τ depends on a diffusion component $\tau_{diffusion}$ dominant in the subthreshold region of operation, and a drift component τ_{drift} valid in the strong inversion region, with the relation given as follows [31]:

$$\frac{1}{\tau} = \frac{1}{\tau_{diffusion}} + \frac{1}{\tau_{drift}} \tag{3}$$

with the two components of τ given by the following expressions [31]

$$\tau_{diffusion} = \frac{qL_{eff}^2}{16\mu_{eff}kT} \tag{4}$$

$$\tau_{drift} = ReC_{ox}W_{eff}L_{eff} \tag{5}$$

with q representing the charge and T representing temperature. The $1/\tau$ based relation is *ipso facto* a frequency oriented relation, and establishes the frequency-oriented charge transport mechanism of the transistor channel.

2

This intuitively justifies how a single transistor can in its natural behavior generate frequency-dependent chaos. Basic Nodal analysis performed for the Elmore equivalent circuit shown in Fig. (3) using Kirchoff Current Law yields a system of coupled equations as follows:

$$V_D Rs + V_S Rd = V_1 Rs + V_2 Rd \tag{6}$$

$$V_G Z_2 + V_G Z_1 = V_1 Z_2 + V_2 Z_1 \tag{7}$$

$$Z_1 = Re + X_{Cdg}; Z_2 = Re + X_{Csg} \tag{8}$$

where X_{Cdg} and X_{Csg} represent the impedances of the source and drain to gate capacitances. The relation for the Elmore Resistance along with the operating point determined by Equation 1, form a system of coupled nonlinear equations, describing the frequency dependent chaotic behavior of a single NMOSFET.
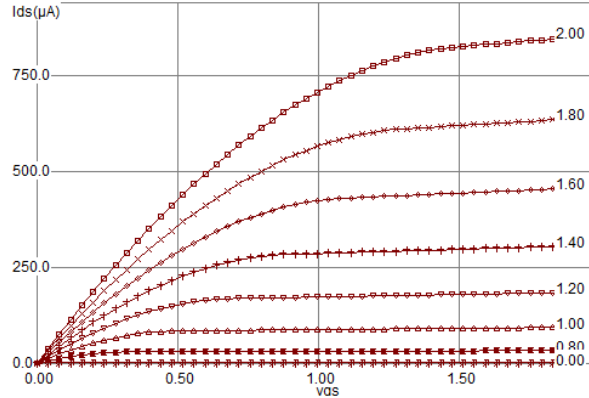
Figure 1: IV Characteristics of a $2\lambda \times 4\lambda$ N-MOSFET in 180nm Technology
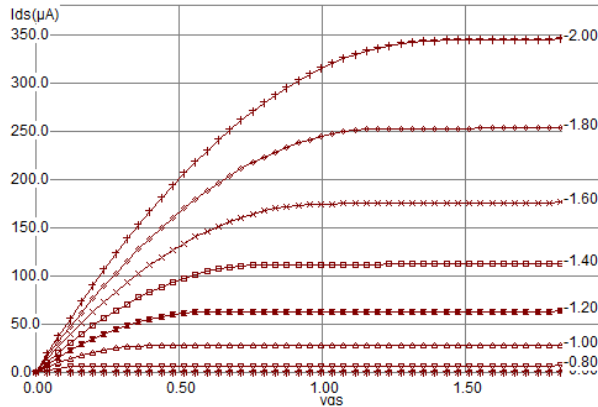
Figure 2: IV Characteristics of a $2\lambda \times 4\lambda$ P-MOSFET in 180nm Technology

Based on these two factors, one can express the nonlinearity of a CMOS Inverter as a Transfer Function between the input V_x connected to the common gate terminal and the output V_y connected to the PMOS source - NMOS drain interconnection [29]. This transfer function for a 180nm CMOS Technology CMOS Inverter with transistors scaled to $2\lambda \times 4\lambda$ is shown in Fig. (4), fitted to a sigmoid function of the following form:

$$V_y = 0.0118 + \frac{0.9646}{1 + 10^{23.0414(V_x - 0.3965)}} \tag{9}$$

From the plot, it can be seen that the key nonlinear transition points of the transfer curve lie at around 0.7V and 1V of the input voltage Vx.

Based on the above mentioned nonlinear behavior of CMOS transistors, the frequency dependent chaos generator circuit is proposed, essentially by coupling two sinusoidal sources to the common gate terminal of a CMOS inverter, as shown in Fig. (5).

3
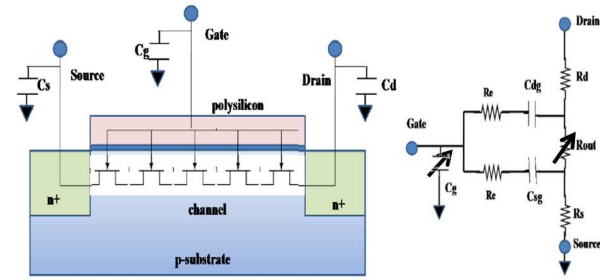
Figure 3: The Non Quasi Static Model of an NMOS Transistor and its equivalent circuit
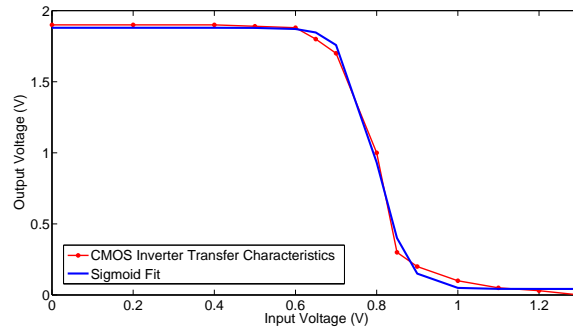
Figure 4: The transfer function of a CMOS Inverter, fitted to a sigmoid
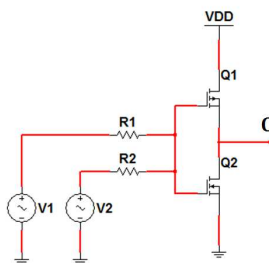
Figure 5: Circuit Schematic of the proposed Chaos Generator

3. 'Frequency Map': The First Perspective

From the schematic shown in Fig. (5), it is clear that the present chaos generator design is based on nonlinearly (due to CMOS) coupling two oscillators (sine sources) with competing frequencies. It is well established in literature that the Circle Map is ideally suited to describing such systems [36, 37, 38, 39, 40]. Thus, this section pertains to the exploration of various aspects of the standard circle map, and the formation and study of the 'frequency map' based on the standard circle map.

3.1. An overview of the Standard Circle Map

Mathematically, the standard circle map is a mapping of the unit circle, demoted as S^1 onto itself, with S^1 parameterized using the angular variable, or phase θ, in the range $[0, 1]$ and expressed as a relative fraction of 360 degrees [36]. Physically, the starting motivation of the standard circle map is a system consisting of two additively coupled oscillators. If the two oscillators are denoted as sine waves having frequencies f_1 and f_2, it is seen that the differences in frequencies cause the phase difference between the sinusoids to grow further and further with each cycle, and this phase difference is seen as the variable θ. Thus, at any instant n, the phase difference at the next instant $n + 1$ depends on the ratio $w = f_2/f_1$ between the two frequencies and is given by the following iterated function, the modulus function signifying the normalization of θ to $[0, 1]$ as mentioned earlier [36].

$$\theta_{n+1} = mod(\theta_n + w, 1) \tag{10}$$

It is seen that for this iterative map, a rational value of w causes a periodic orbit, whereas in an irrational case, the sequence of θ_n is seen to densely occupy the space defined by $[0, 1]$, thus giving rise to a 'quasiperiodic' regime of operation [36].

Arnold made a slight modification to the above mentioned iterated function by adding a nonlinear coupling term, resulting in the following map, termed 'The Standard Circle Map' [38].

$$\theta_{n+1} = mod(\theta_n + w + \frac{K}{2\pi}sin(2\pi\theta_n), 1) \tag{11}$$

The addition of the third term in the iterated function enables the control of the system behavior beyond periodic and quasiperiodic regimes using K. This map can be studied as two regions, K below 1 and K above 1, as follows:

1. When K is varied from 0 to 1, it is seen that the circle map becomes a perfect homeomorphism of S^1 onto itself. In such a case, the behavior of the circle map depends on the rotation number R, a function of w and K defined as follows [43, 44, 45, 46]:

$$R = \lim_{N \to \infty} \frac{1}{N} \sum_{n=0}^{N-1} [w + \frac{K}{2\pi}sin(2\pi\theta_n)] \tag{12}$$

   An irrational value of R renders the circle map equivalent to a pure rotation corresponding to the quasiperiodic case, whereas a rational value of R causes a periodic orbit with periodic points on the unit circle similar to the pure rotation case [38]. For small denominator f_1, regions of frequency locking, termed 'Arnold's Tongues' are observed on the (w, K) plane [36, 38, 43, 44, 45, 46]. The nature of dynamics varies from purely quasiperiodic at $K = 0$ to a peculiar 'Devil's Staircase' pattern at $K = 1$ [38].

2. When K is greater than unity, noninvertible behavior is observed, leading to chaos. The Standard Circle Map is seen to have negative sloped branches, where negative slopes greater than -1 give rise to cascades of period doubling leading to chaos [36].In this scenario, the rotation number depends on the initial conditions, a defining property of chaos.

3.2. The Frequency Map

The key objective in defining the 'frequency map' from the circle map is to transfer the control of chaos from a system related coupling parameter K to a signal based parameter r.

As a starting step, the Standard Circle Map mentioned above is viewed as a purely mathematical relation and θ is written as $f_o t$ where f_o represents the normalized version of the angular frequency, given in the units of radians/sample, with a full scale range of $-\pi$ to π.

Also, the time factor t is set to one, representing one sample duration, between the ith and $i + 1$th instants. The additive parameter w is rewritten as r where $r=f_2/f_1$ is the ratio between two normalized competing driving frequencies f_1 and f_2 and is the principal control parameter for the present work. The value of K is arbitrarily set to 2π in order to set the coefficient of the third term of the above equation to unity. It is noted that the value 2π set to K is above unity,

and is thus a chaos generating value. Finally, the sinusoid $sin(2\pi\theta(i))$ is viewed as a mathematical function representing the input signal and is generalised to $V(2\pi f_o(i))$, or alternatively $V(f_o(i))$, with V representing the signal waveform fed to the input of the proposed chaotic system. Using these substitutions, the above equation is rewritten as follows.

$$f_o(i+1) = mod(f_o(i) + r - V(f_o(i)), 1) \tag{13}$$

It is highlighted at this stage that, by making the various modifications to the standard circle map, its physical significance is altered considerably, and it now takes a new form represented by frequency variables and input signal dependence. In order to retain the consistency of the above equation, the various terms are normalized to π. First, the frequency f_o and the frequencies f_1 and f_2 are normalized to the radians/sample scale of $[-\pi, \pi]$. Finally, the term $V(f_o(i))$ is limited to π, i.e. 3.14 Volts by changing the modulus function from 1 to π, a value comprehensively encompassing the linear and saturation operating regions of the transistor, as well as forms a convenient normalizing factor yielding effective integration of the frequency and voltage terms. At this point, it is observed that the f and V terms of the above equation are merely reduced to normalized mathematical numbers. Thus, the normalized version of the above equation, with the f and V terms limited to π using a modulus function is given as follows:

$$f_o(i+1) = mod(f_o(i) + \frac{f_2}{f_1} - V(f_o(i)), \pi) \tag{14}$$

This iterated function is termed 'The Frequency Map' and forms the first perspective of single CMOS inverter chaos generation in the present work.

Here the f_o terms denote the output frequencies, whereas f_1 and f_2 denote the frequencies of the input (driving) signals. $V(f_o)$ denotes the input signal waveform employed in the chaotic system.

The key components of the obtained frequency map are threefold, enumerated as follows:

1. The nonlinearity, provided by the modulus function represents the CMOS inverter switching operation, operating in the cutoff and saturation regions.
2. The control parameter $r=f_2/f_1$ is an additive parameter and determines when the system transits from order to chaos and vice versa.
3. The $V(f_o)$ introduces a signal dependence, thus enabling the controlling of chaos by changing the waveform used as input. For instance, in the case of sinusoidally driven system, $V(f_o)$ becomes $sin(f_o(i))$ which can be decomposed into a power series containing the odd powers of $(f_o(i))$. Thus, the signal dependance introduces nonlinearity in addition to the system nonlinearity obtained by the switching function.

The frequency map derived above can be studied using standard tools such as the Bifurcation and Cobweb Plots. The Bifurcation plot is a plot showing the values of output parameter $f_o(i)$ as a function of the control parameter r [3, 4]. Thus, the bifurcation plot shows the transitions from order, represented by less 'crowded' values of r to chaos, seen as densely 'crowded' and 'grassy' regions of r and vice versa [3, 4]. The bifurcation plot for the proposed Frequency Map is shown in Fig. (6) for r ranging from 0 to 2, from which two key inferences can be derived:

1. The pattern is periodic, since it repeats itself with a period of 1.
2. The control values of r close to integers (1,2,...) and half-integers (0.5, 1.5,...) give rise to more orderly and quasiperiodic behavior whereas non integral ratios such as 0.22 or 0.41 for instance give rise to chaos.
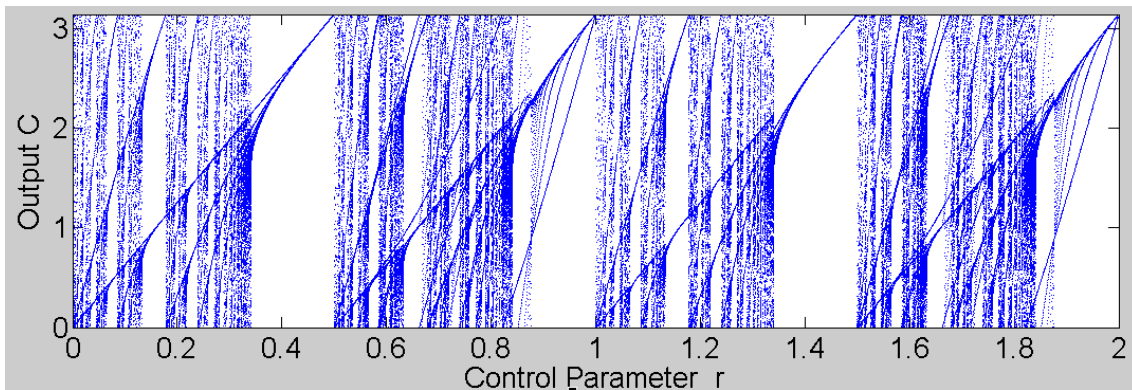
Figure 6: Bifurcation plot of the Frequency Map

While the bifurcation plot depicts the output $f_o(i)$ as a function of r, a plot that graphically visualizes the successive iterations of $f_o(i)$ for a fixed r is the Cobweb Plot [3, 4]. This plot is shown in Fig. (7), Fig. (8) and Fig. (9) for an integer r of 10, rational r of 10.7 and an irrational r of 3.4π respectively. It is seen that the r values corresponding to more chaotic regions in the bifurcation plots show spaced out and denser non-repetitive patterns in the cobweb plots.
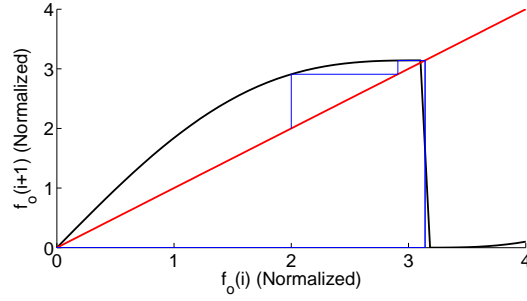
Figure 7: Cobweb plot of the frequency map for $r = 10$
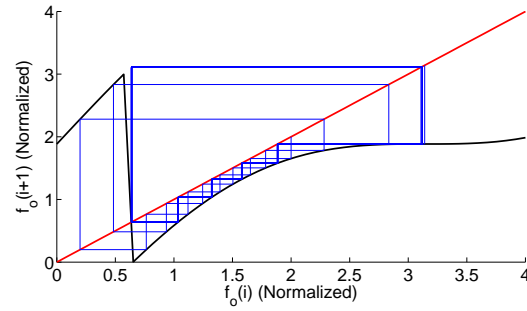
Figure 8: Cobweb plot of the frequency map for $r = 10.7$
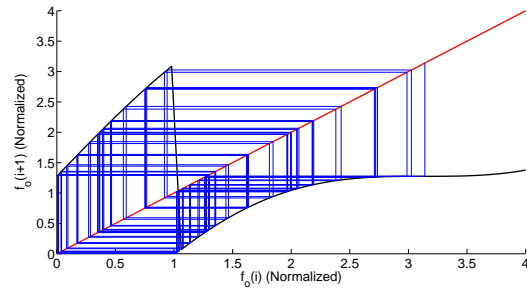
Figure 9: Cobweb plot of the frequency map for $r = 3.4\pi$

4. 'Amplitude Map': The Second Perspective

In order to form an amplitude map for the schematic of Fig. (5), the sigmoid representing the CMOS Inverter transfer function, shown in Equation 3 is considered. Output Variable V_y is replaced with C representing the chaotic output, and the input variable V_x is replaced as the sum of two sinusoids, with the rewritten equation as follows. For the sake of convenience, the amplitudes of both sinusoids are set equal at 'A'.

$$C = 0.0118 + \frac{0.9646}{1 + 10^{23.0414(Asin(2\pi f_1 t) + Asin(2\pi f_2 t) - 0.3965)}} \tag{15}$$

The amplitude map can be written in terms of the time derivative of C, by converting it into a difference equation as follows:

$$\frac{dC}{dt} = C_{n+1} - C_n \tag{16}$$

$$C_{n+1} = C_n - \frac{51.1766[2A\pi f_1 cos(2\pi f_1 t) + 2Ar\pi f_1 cos(2\pi r f_1 t)]10^{23.0414(Asin(2\pi f_1 t)+Asin(2\pi r f_1 t)-0.3965)}}{1 + 10^{23.0414(Asin(2\pi f_1 t)+Asin(2\pi f_1 rt)-0.3965^2}} \tag{17}$$

Based in this, the 'Amplitude Map' is obtained as in Equation 9.

It is seen that this Amplitude Map incorporates the Nonlinearity of the CMOS transistors through the sigmoid function, while also preserving the signal based nonlinearity denoted by the f_1 and r terms.

As was the case with the frequency map, the amplitude map is analyzed by plotting a bifurcation plot with r ranging from 0 to 10, and is shown in Fig. (10) for a A value of 0.2. It is seen that the bifurcation plot shows multiple overlapping 'lobes' with varying widths. Certain non chaotic points such as the one with $r = 3$ can be discerned from the ornamental pattern. However, for larger values of A, such as 0.4, 'purely chaotic' amplitude maps can be obtained, as shown in Fig. (11), where regions of non-chaotic order are almost non-existent [47, 48, 49].
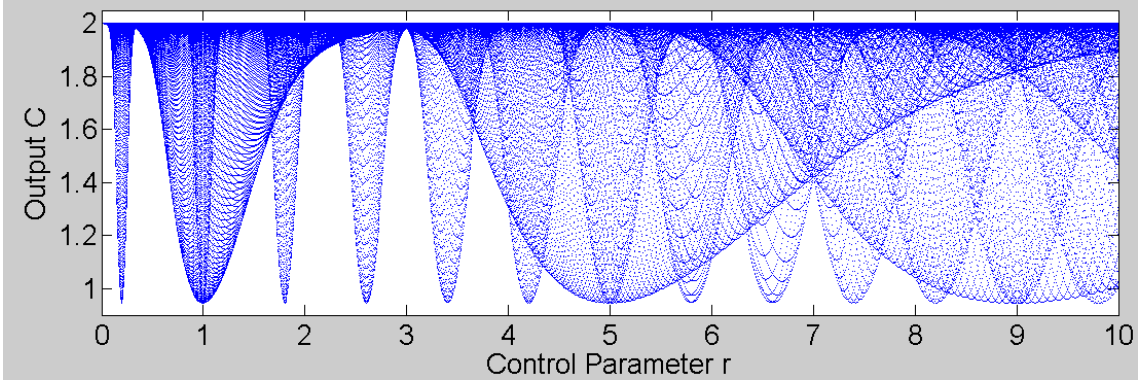
Figure 10: Amplitude Map Bifurcation Plot for $A = 0.2$
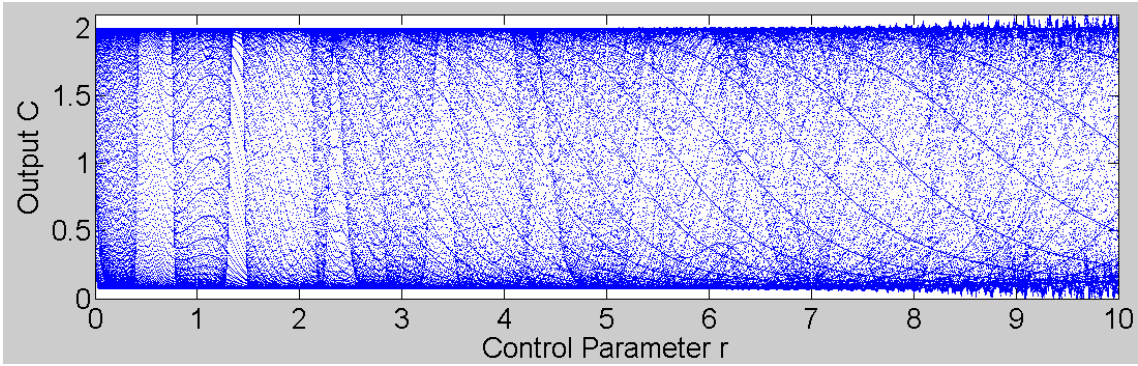
Figure 11: Amplitude Map Bifurcation Plot for $A = 0.4$

A key tool to analyze the chaotic behavior in an amplitude map is the phase portrait, which displays the derivative dC/dt as a function of C. This plot describes the stability aspects of the chaotic system behavior and points of stability around which the system revolves, qualitatively serving as a tool to assess various chaotic parameters such as sensitivity and ergodicity [3, 4]. Based on the Amplitude Map of Equation 17, r is set to π, and the phase portraits for $A = 0.2$ and $A = 0.4$ are shown in Fig. (12) and Fig. (13) respectively. It is seen that for a higher value of A, the phase portrait is much more dense and ornamental, testifying to the 'purely chaotic' bifurcation map seen earlier.

5. Implementation in Hardware

The validation of the Frequency and Amplitude Maps is carried out by implementing the circuit schematic of Fig. (5) in hardware using MTP50 series low frequency transistors, using the setup shown in Fig. (14). In order to validate
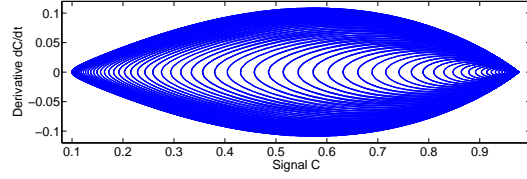
Figure 12: Amplitude Map Phase portrait for $A = 0.2$
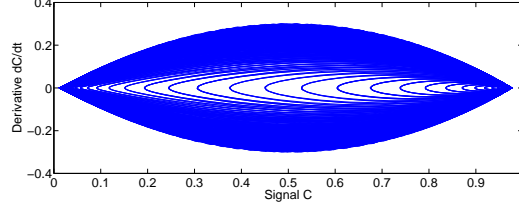
Figure 13: Amplitude Map Phase portrait for $A = 0.4$

the amplitude map, the phase portrait of the output signal for $A = 0.4$ and $r = \pi$ is plotted in Fig. (15). The similarity with the theoretically obtained phase portrait of Fig. (13) is clearly evident.

In order to validate the frequency map, the Fourier Spectra (FFT) of the generated chaotic output is plotted in Fig. (16), Fig. (17) and Fig. (18) for r values of 10, 10.7 and 3.4π respectively. It is seen that the trends of the spectra are in accordance with the cobweb plots of Fig. (7), Fig. (8) and Fig. (9), with denser cobweb plots corresponding to more chaotic regions in Fig. (6) and consequently having denser frequency components in FFT Spectra.
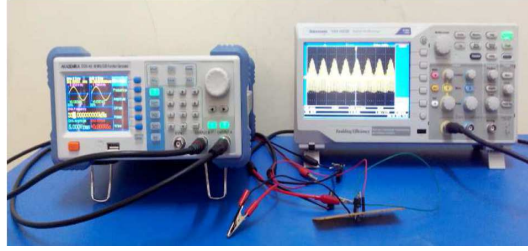
Figure 14: Experimental setup for generation of frequency dependent chaos
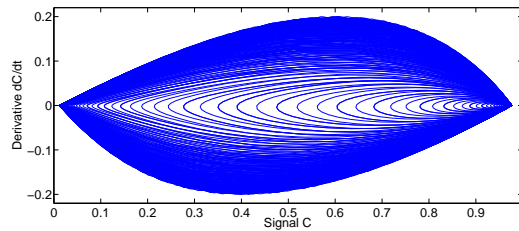
Figure 15: Experimentally obtained Phase portrait for $A = 0.4$

The chaotic nature of the obtained signal C is assertively established by calculating the largest Lyapunov Exponent (LLE), a measure of a system's sensitive dependence on initial conditions [41, 42]. Rosenstein's algorithm is used to compute the Lyapunov Exponents λ_i from the voltage waveform, where the sensitive dependence is characterized by the divergence samples $d_j(i)$ between nearest trajectories represented by j given as follows, C_j being a normalization constant [41, 42]:

$$d_j(i) = C_j e^{\lambda_i (i\delta t)} \tag{18}$$

The Largest Lyapunov exponent thus obtained for the chaotic signal is 9.385 for an r value of π, the positive value proving the fact that the signal is indeed chaotic.

9
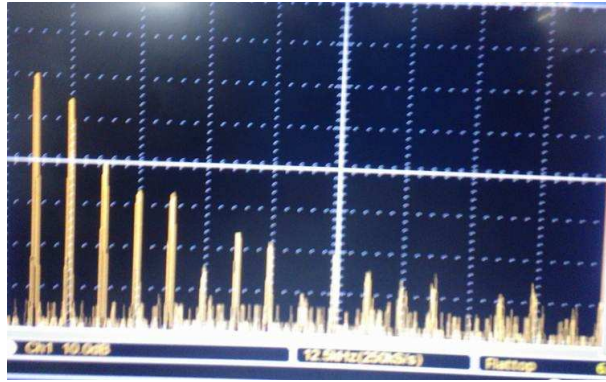
Figure 16: Output Signal FFT Spectrum for $r = 10$
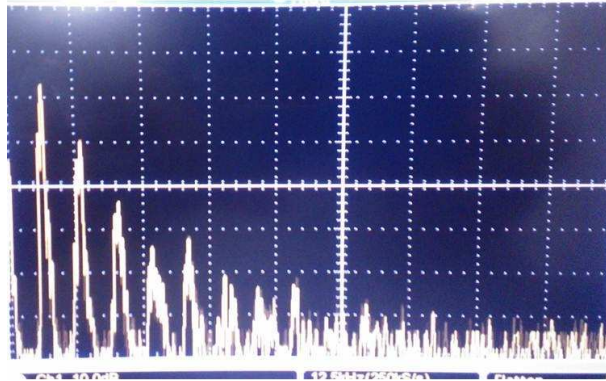
Figure 17: Output Signal FFT Spectrum for $r = 10.7$
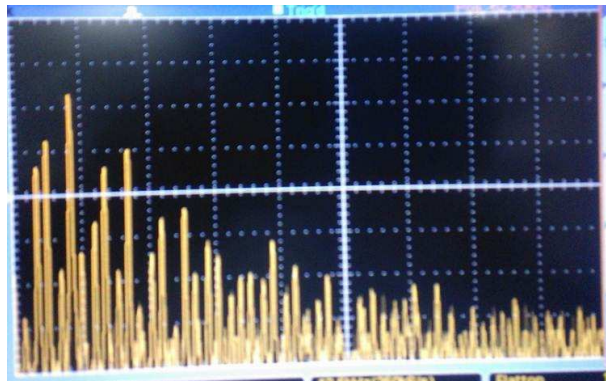
Figure 18: Output Signal FFT Spectrum for $r = 3.4\pi$

The worthiness of the generated signal as a potential candidate as a carrier for secure communications can be established by ascertaining the amount of information that can be carried by the signal. This is precisely quantified by the Kolmogorov Entropy, a statistical measure of the uncertainty of the signal [41, 42]. By assigning each of the N quantifiable states of the amplitude of C as an event i, the Kolmogorov Entropy K_2 obtained depends on their probabilities p_i according to the relation [41, 42]

$$K_2 = -\sum_{i=1}^{N} p_i \log p_i \tag{19}$$

Since the chaotic output waveform is a continuously varying amplitude, a very high value of N such as 100000 is selected as the number of quantifiable states. Thus, the presence of each of the N states is viewed as an event p_i. The K_2 value thus obtained is 3.96 bits/symbol, clearly testifying to the information carrying capacity of the generated chaotic signal C.

According to the basic premise of the proposed frequency dependent chaos, as witnessed by the iterative map and bifurcation diagrams described earlier, the nature of the chaos generated depends on the frequency of the driving signal. Various of frequency ratio r ranging from 1 to 2 in steps of 0.1 are implemented, and the corresponding parameters of LLE, K_2 are tabulated in Table 1. From the table, it is observed that the frequency of the driving signals indeed affect the nature of chaos generated, and the trend reflects the one seen in the bifurcation diagram of Fig. (6). For this reason, the generated chaos is termed 'Frequency Dependent Chaos'.

Table 1: Effect of r on the Generated Chaos

Ratio r	LLE	K_2 (bits/sym)
1.1	9.18	6.67
1.2	10.01	6.92
1.3	9.84	6.87
1.4	9.57	6.81
1.5	9.17	6.77
1.6	9.21	6.79
1.7	9.89	6.88
1.8	9.66	6.82
1.9	9.12	6.73

6. Conclusion

After exploring the nonlinear behavior of a CMOS inverter, a novel approach to generation of chaos using single CMOS inverter is proposed. The theoretical basis for the proposed circuit is explored in two perspectives. The first perspective corresponds to frequency, viewing the chaos generator as a nonlinear coupling of two oscillations with competing frequencies. Based on this premise, the Standard Circle Map is studied and a Frequency Map describing the chaos generator is derived from it. The trends of this map are explored using bifurcation and cobweb plots. Following this, the second perspective, based on amplitude is discussed. A sigmoid function describing the CMOS inverter transfer characteristics is taken and by adapting its derivative to a difference equation, an amplitude iterative map is formed. This map is studied using the bifurcation plot and phase portraits. Finally, an experimental implementation of the proposed chaos generator is performed, and the phase portraits and FFT spectrum trends are seen to agree with the theoretical models described earlier. Nonlinear characterization of the generated output signal is performed using Lyapunov Exponents and Kolmogorov Entropy. In conclusion, it is seen that the frequency dependent chaos proposed in the present work offers a radical shift from system oriented chaos generation to signal oriented chaos generation, with the obvious advantages of easy tunability and simplicity of design, which form the novelty of the present work.

References

[1] G. B. Giannakis, F. Bach, R. Cendrillon, M. Mahoney,J. Neville, *Signal Processing for Big Data*, IEEE Signal Processing Magazine, **31**, 15-16 (2014).

[2] M. Hilbert, *How much of the global information and communication explosion is driven by more, and how much by better technology?*, Wiley Journal of the Association for Information Science and Technology, **65**, 856-861 (2014).

[3] M. Ausloos, M. Dirickx, *The Logistic Map and the Route to Chaos: From the Beginnings to Modern Applications*, (Springer, US, 2006).

[4] S. H. Strogatz, *Nonlinear Dynamics and Chaos: With Applications to Physics, Biology, Chemistry, and Engineering* ,(Westview Press, Cambridge, 2008).

[5] A. Kudrolli, A, J. P. Gollub. *Patterns and spatiotemporal chaos in parametrically forced surface waves: a systematic survey at large aspect ratio.* Physica D: Nonlinear Phenomena **97**, 133-154 (1996).

[6] J. Briggs, *Fractals: The patterns of chaos: A new aesthetic of art, science, and nature.* (Simon and Schuster, 1992).

[7] M. Lakshmanan, S. Rajaseekar, *Nonlinear dynamics: integrability, chaos and patterns.* (Springer Science and Business Media, 2012).

[8] I R. Epstein, K. Showalter. *Nonlinear chemical dynamics: oscillations, patterns, and chaos.* The Journal of Physical Chemistry **100** 13132-13147 (1996).

[9] M. H. Jensen, P. Bak, T. Bohr, *Complete Devil's Staircase, Fractal Dimension, and Universality of Mode- Locking Structure in the Circle Map*, Phys. Rev. Lett. **50**, 1637 (1983).

[10] F. Cramer, *Chaos and Order the Complex Structure of Living Systems.* (Springer, 1993).

[11] D. S. Coffey, *Self-organization, complexity and chaos: the new biology for medicine.* Nature medicine **4**, 882-885 (1998).

[12] G. Contopoulos, *Order and chaos in dynamical astronomy*, (Springer Science and Business Media, 2002).

[13] J. Laskar, *Large-scale chaos in the solar system."*, Astronomy and Astrophysics **287**, L9-L12 (1994).

[14] A. B. Cambel, *Applied chaos theory-A paradigm for complexity.* (Academic Press, Inc., 1993).

[15] K. Aihara, *Chaos engineering and its application to parallel distributed processing with chaotic neural networks.* Proceedings of the IEEE, **90** 919-930 (2002).

[16] G. Chen, *Controlling chaos and bifurcations in engineering systems.* (CRC press, 1999).

[17] R. B. Stull, *An introduction to boundary layer meteorology.* (Springer Science and Business Media, 1988).

[18] M. F. Barnsley, A. D. Sloan, *Chaotic Compression*, Computer Graphics World, **3** (1987).

[19] K. E. Barner G. R. Arce, *Nonlinear Signal and Image Processing: Theory, Methods, and Applications*, (CRC Press, U.S, 2003).

[20] S. Saini, J. S. Saini. *Secure communication using memristor based chaotic circuit.* Parallel, Distributed and Grid Computing (PDGC), 2014 International Conference on. IEEE, (2014).

[21] S. Shaerbaf, S. A. Seyedin. *Nonlinear Multiuser Receiver for Optimized Chaos-Based DS-CDMA Systems.*, Iranian Journal of Electrical andElectronic Engineering **7**, 149 (2011): 149.

[22] L. Kocarev, *From chaotic maps to encryption schemes.* Circuits and Systems, (1998).

[23] G. Jakimoski, L. Kocarev. *Chaos and cryptography: block encryption ciphers based on chaotic maps.* IEEE Transactions on Circuits and Systems I: Fundamental Theory and Applications **48** 163-169 (2001).

[24] E.Bilotta and P.Pantano, *A gallery of Chua attractors*, (World Scientific, Singapore, 2008).

[25] L. Chua, *A universal circuit for studying and generating chaos. I. Routes to chaos.* Circuits and Systems I: Fundamental Theory and Applications, IEEE Transactions on **40**732-744 (1993).

[26] G. Kolumban, M. P. Kennedy, L. O. Chua. *The role of synchronization in digital communications using chaos. II. Chaotic modulation and chaotic synchronization*, Circuits and Systems I: Fundamental Theory and Applications, IEEE Transactions on **45**, 1129-1140 (1998).

[27] L. Chua, *Chaos synchronization in Chua's circuit*, Journal of Circuits, Systems, and Computers **3**, 93-108 (1993).

[28] L. Chua, *Experimental chaos synchronization in Chua's circuit.* International Journal of Bifurcation and Chaos **2**, 705-708 (1992).

[29] B. Razavi, *RF Microelectronics*, (Prentice Hall, US, 2011).

[30] B. G. Streetman and S. K.Banerjee, *Solid State Electronic Devices*, (PHI, U.S, [2006]).

[31] M.Chan, K.Hui, C.Hu, P.K.Ko, *A robust and physical BSIM3 non quasi static transient and AC small signal model for circuit simulation*, IEEE Transactions on Electron Devices. **45**, 834 (1998).

[32] M. E. Inchiosa, A. R. Bulsara, A. D. Hibbs, B. R. Whitecotton, *Signal Enhancement in a Nonlinear Transfer Characteristic*, Phys. Rev. Lett. **80**, 1381 (1998).

[33] F. Balestra, *Nanoscale CMOS: Innovative Materials, Modeling and Characterization* (Wiley,US, [2013]).

[34] W.Liu, *BSIM 4.0.0 MOSFET Model: User's Manual* (Electronics Research Laboratory,US, [2000]).

[35] J. P. Uyemura, *Chip Design for Submicron VLSI: CMOS Layout and Simulation*, (Thomson/Nelson, US, [2006]).

[36] R. Gilmore, M. Lefranc, *The Topology of Chaos*, (Wiley,US, [2002]).

[37] J. M. T. Thompson, H. B. Stewart, *Nonlinear Dynamics and Chaos* (Wiley,UK, [2002]).

[38] V. I. Arnold, *Small Denominators I. Mappings of the circumference onto itself*, Am. Math. Soc. Transl, **46**, 213-284 (1965).

[39] M. R. Hermann, *Mesure de Lebesgue et nobre de rotation (Geometry and Topology)*, (Springer,Germany, [1977]).

[40] R. S. Mackay and C. Tresser, *Some flesh on the skeleton: the bifurcation structure of bimodal maps*, J. Phys. Lett., **45**, L741-L746 (1984).

[41] R. G. James, K. Burke, J. P. Crutchfield, *Chaos forgets and remembers: Measuring information creation, destruction, and storage*, Int. J Bifurcation Chaos. **378**, 2124 (2014).

[42] M. T. Rosenstein, J. J. Collins, C. J. De Luca, *A practical method for calculating largest Lyapunov exponents from small data sets*, Physica D, **65**, 117, (1993).

[43] A. Katok, B. Hasselblatt. *Introduction to the Modern Theoy of Dynamical Systems.* (Cambridge University Press, 1995).

[44] R. L. Devaney. *An Introduction of Chaotic Dynamical Systems.* (Addison-Wesley, 1989).

[45] J. Guckenheimer and P. H. Holmes. *Nonlinear Oscillators, Dynamical Systems and Bifurcations of Vector Fields.* (Springer-Verlag, 1986).

[46] V. 1. Arnold. *Ordinary Diferential Equations.* (MIT Press, 1989).

[47] R. M. May, *Regulation of populations with nonoverlapping generations by microparasites: a purely chaotic system*, American Naturalist, **85**, 573-584, (1985).

[48] U. S. Freitas, C. Letellier, L. A. Aguirre, *Failure in distinguishing colored noise from chaos using the noise titration technique*, Physical Review E, **79**, 035201, (2009).

[49] F. Doveri, M. Scheffer, S Rinaldi, S. Muratori, Y. Kuznetsov, *Seasonality and chaos in a plankton fish model*, Theoretical Population Biology, **43**, 159-183, (1993).